

Dynamic Consistency in a Predator–Prey Model with Habitat Complexity: Nonstandard Versus Standard Finite Difference Methods

N. Bairagi

Centre for Mathematical Biology and Ecology
Jadavpur University
Department of Mathematics
Kolkata-700032, India
nbairagi@math.jdvu.ac.in

M. Biswas

Department of Mathematics
A. J. C Bose College
A. J. C Bose Road, Kolkata-700020, India
milanju10@gmail.com

Abstract

In this paper, we discretize a continuous time predator–prey model that considers the effect of habitat complexity following nonstandard finite difference (NSFD) method as well as the standard forward Euler method. We study the positivity of the solutions, stability and instability of different fixed points of both systems. It is shown that the model formulated by NSFD method shows complete dynamic consistency with its continuous counterpart, but the standard discrete model does not. In fact, the latter system shows spurious dynamic behavior. Moreover, the qualitative behavior of the NSFD system is independent of the step size, whereas the behavior of the Euler system depends on the step size. Extensive numerical experiments have also been performed in support of our analytical results.

AMS Subject Classifications: 37N25, 39A30, 92B05, 92D25, 92D40.

Keywords: Nonstandard finite difference scheme, Euler’s scheme, dynamic consistency, predator–prey model, habitat complexity, stability, oscillations.

1 Introduction

The general predator–prey model in its classical form is represented by

$$\begin{aligned}\dot{x} &= xf(x) - yg(x), \\ \dot{y} &= \theta yg(x) - dy,\end{aligned}\tag{1.1}$$

where $x(t)$ and $y(t)$ are the densities of prey and predator populations at time t , respectively. $f(x)$ is the per capita growth rate of prey in absence of predator and d is the food-independent predator mortality rate. $g(x)$ is the functional response of predator, which is defined as the number of prey caught per predator per unit of time. The term $\theta g(x)$ is known as the numerical response, measuring the number of newly born predators for each captured prey and θ ($0 < \theta < 1$) is the conversion efficiency.

It has been demonstrated that physical or structural complexity of habitat plays significant role in local population communities [3, 7, 17, 18, 27, 28, 43]. Habitat structure is defined as any biotic and abiotic physical structure in space, whereas habitat structural complexity refers to the morphological characteristics within a structure itself or the heterogeneity in the arrangement of objects in space [6, 30]. Habitat complexity is found in almost all ecological systems, whether it is terrestrial or aquatic. Marine habitat, in particular, becomes complex in presence of oyster and coral reefs, mangroves, sea grass beds and salt marshes [23]. Empirical and experimental results suggest that habitat complexity plays a significant role in the predator–prey dynamics. It has been demonstrated that structural complexity of the habitat stabilizes the predator–prey interaction between piscivorous perch (predator) and juvenile perch and roach (prey) by reducing predator foraging efficiency [37–39]. Luckinbill [31] and Veilleux [44] prolonged the coexistence of *Paramecium aurelia* (prey) and *Didinium nasutum* (predator) in laboratory system by using Methyl Cellulose in the Cerophyl medium (nutrient). However, both paramecium and didinium go to extinction in absence of Methyl Cellulose [14, 16, 22]. The general hypothesis is that there exists an inverse relationship between predation rate and the degree of habitat complexity [9, 15, 17, 23, 41]. Therefore, effect of habitat complexity should be incorporated in predator’s response function when theoretical models are used to study predator–prey interaction. However, the traditional mathematical models have understated the role of habitat complexity in understanding predator–prey dynamics.

The most commonly used functional response in a predator–prey model is Holling Type II and is mathematically represented by $g(x) = \frac{\alpha x}{1 + \alpha h x}$, where α is the attack coefficient, h is the handling time. This response function does not incorporate the effect of habitat complexity. So the formula cannot be used directly as predation formula when complexity is present in the habitat. To incorporate the effect of habitat complexity, the Type II functional response was modified as $g(x) = \frac{\alpha(1-c)x}{1 + \alpha(1-c)hx}$, where the dimensionless parameter c ($0 < c < 1$) measures the degree or strength of habitat complexity [4, 5, 24, 25]. If the prey population follows density-dependent logistic growth

with intrinsic growth rate r , carrying capacity k , and predation process obeys modified Type II response function, then the system (1.1) in presence of habitat complexity reads as [5]

$$\begin{aligned}\frac{dx}{dt} &= rx \left(1 - \frac{x}{k}\right) - \frac{\alpha(1-c)xy}{1 + \alpha h(1-c)x}, \\ \frac{dy}{dt} &= \frac{\theta\alpha(1-c)xy}{1 + \alpha h(1-c)x} - dy.\end{aligned}\tag{1.2}$$

Conventional discretized models generally exhibit richer and more complicated dynamical behaviors than its corresponding continuous models [13]. The reason is that such discretized models are formulated by traditional schemes like forward and backward Euler, Runge–Kutta, Adams methods. Euler forward method is most popularly used to study the discrete version of a continuous model [20, 21, 26]. Such discretized models produce spurious behaviors like oscillations, bifurcations and chaos [29]. However, the corresponding continuous system may not show such complex dynamics. One alternative to prevent this dynamical inconsistency is the construction of discrete models using nonstandard finite difference method developed by Mickens [35]. The NSFD scheme has been successfully used to different real-life models to avoid spurious solutions of standard difference models [1, 11, 33, 36, 42, 45]. One of the most important aspects of NSFD scheme is that each differential equation has to be considered as a unique mathematical structure and consequently must be discretely modeled in a unique manner [32]. In this paper, we seek to construct a discrete model of the corresponding continuous model (1.2) that preserves the qualitative properties of the continuous system and maintains dynamic consistencies. We would also like to compare these results with the results of the Euler method.

The organization of this paper is as follows. In Section 2, we state some basic definitions and summarize the results of the continuous system. Two discrete systems and their qualitative behaviors are presented in Section 3. Extensive numerical simulations are presented in Section 4 to substantiate and compare our analytical results. Finally, we summarize the results in Section 5.

2 Some Definitions and Results of the Continuous System

Consider the differential equation

$$\frac{dx}{dt} = f(x, t, \lambda),\tag{2.1}$$

where λ represents the parameter defining the system (2.1). Assume that a finite difference scheme corresponding to the continuous system (2.1) is described by

$$x_{k+1} = F(x_k, t_k, h, \lambda).\tag{2.2}$$

We assume that $F(., ., .)$ is such that the proper uniqueness–existence properties holds; the step size is $h = \nabla t$ with $t_k = hk$, $k = \text{integer}$; and x_k is an approximation to $x(t_k)$.

Definition 2.1 (See [34]). Let the differential equation (2.1) and/or its solutions have a property P . The discrete model (2.2) is said to be dynamically consistent with the equation (2.1) if it and/or its solutions also have the property P .

Definition 2.2 (See [2, 10, 34]). The NSFD procedures are based on just two fundamental rules:

- (i) The discrete first derivative has the representation $\frac{dx}{dt} \rightarrow \frac{x_{k+1} - \psi(h)x_k}{\phi(h)}$, $h = \Delta t$, where $\phi(h)$, $\psi(h)$ satisfy the conditions $\psi(h) = 1 + O(h^2)$, $\phi(h) = h + O(h^2)$.
- (ii) Both linear and nonlinear terms may require a nonlocal representation on the discrete computational lattice. For example,

$$x \rightarrow 2x_k - x_{k+1}, \quad x^3 \rightarrow \left(\frac{x_{k+1} + x_{k-1}}{2} \right) x_k^2,$$

$$x^3 \rightarrow 2x_k^3 - x_k^2 x_{k+1}, \quad x^2 \rightarrow \left(\frac{x_{k+1} + x_k + x_{k-1}}{3} \right) x_k.$$

While no general principles currently exist for selecting the functions $\psi(h)$ and $\phi(h)$, particular forms for a specific equation can easily be determined. Functional forms commonly used for $\psi(h)$ and $\phi(h)$ are

$$\phi(h) = \frac{1 - e^{-\lambda h}}{\lambda}, \quad \psi(h) = \cos(\lambda h),$$

where λ is some parameter appearing in the differential equation.

Definition 2.3. The finite difference method (2.2) is called positive if for any value of the step size h , solution of the discrete system remains positive for all positive initial values.

Definition 2.4. The finite difference method (2.2) is called elementary stable if for any value of the step size h , the fixed points of the difference equation are those of the differential system and the linear stability properties of each fixed point being the same for both the differential system and the discrete system.

Definition 2.5 (See [12]). A method that follows the Mickens rules (given in the Definition 2.2) and preserves the positivity of the solutions is called positive and elementary stable nonstandard (PESN) method.

The following properties are known for the ODE system (1.2) [5].

- (I) Positivity and boundedness: Solutions of this system are positive and bounded when start with positive initial values.
- (II) Equilibrium points and their existence: The continuous system (1.2) has three fixed points. The trivial fixed point $E_0(0, 0)$ and the predator-free fixed point $E_1(k, 0)$ always exist. The coexistence fixed point is described by $E^*(x^*, y^*)$, where $x^* = \frac{d}{\alpha(1-c)(\theta-hd)}$ and $y^* = \frac{r(k-x^*)[1+h\alpha(1-c)x^*]}{k\alpha(1-c)}$. It exists if $\theta > hd$ and $c < c_0$, where $c_0 = 1 - \frac{d}{k\alpha(\theta-hd)}$.
- (III) Local stability of the equilibrium points: The fixed point E_0 is a saddle point. The predator-free fixed point E_1 is a saddle point if $c < c_0$ and stable if $c > c_0$. In the latter case, the coexistence fixed point E^* does not exist. The fixed point E^* is stable if (i) $\alpha > \frac{1+hd}{kh(1-hd)}$, (ii) $\frac{hd(\alpha kh+1)}{(\alpha kh-1)} < \theta < 1$ and (iii) $c_1 < c < c_0$, where $c_1 = 1 - \frac{\theta+hd}{\alpha kh(\theta-hd)}$, $c_0 = 1 - \frac{d}{\alpha k(\theta-hd)}$ and unstable for $0 < c < c_1$. A Hopf bifurcation exists at $c = c_1$.

3 Study of Discrete Models

In the following, we propose two discrete models formulated by nonstandard finite difference (NSFD) technique introduced by Mickens and Euler forward method and study their dynamical behaviors.

3.1 Nonstandard Finite Difference Method

For convenience, we first express the continuous system (1.2) as follows:

$$\begin{aligned} \frac{dx}{dt} &= rx - \frac{r}{k}x^2 - P(x, y)x, \\ \frac{dy}{dt} &= Q(x)y - dy, \end{aligned} \tag{3.1}$$

where $P(x, y) = \frac{\alpha(1-c)y}{1+\alpha h(1-c)x}$ and $Q(x) = \frac{\theta\alpha(1-c)x}{1+\alpha h(1-c)x}$. We employ the following nonlocal approximations termwise for the system (3.1):

$$\begin{cases} \frac{dx}{dt} \rightarrow \frac{x_{n+1} - x_n}{t}, & \frac{dy}{dt} \rightarrow \frac{y_{n+1} - y_n}{t}, \\ x \rightarrow 2x_n - x_{n+1}, & Q(x)y \rightarrow Q(x_{n+1})(2y_n - y_{n+1}), \\ x^2 \rightarrow x_n x_{n+1}, & y \rightarrow y_{n+1}, \\ P(x, y)x \rightarrow P(x_n, y_n)x_{n+1}, \end{cases} \tag{3.2}$$

where $t (> 0)$ is the stepsize.

By these transformations, the continuous-time system (1.2) transforms to the system

$$\begin{aligned}\frac{x_{n+1} - x_n}{t} &= r(2x_n - x_{n+1}) - \frac{r}{k}x_nx_{n+1} - \frac{\alpha(1-c)y_nx_{n+1}}{1 + \alpha h(1-c)x_n}, \\ \frac{y_{n+1} - y_n}{t} &= \frac{\theta\alpha(1-c)x_{n+1}(2y_n - y_{n+1})}{1 + \alpha h(1-c)x_{n+1}} - dy_{n+1}.\end{aligned}\quad (3.3)$$

The above system can be rewritten as

$$\begin{aligned}x_{n+1} &= \frac{(1 + 2rt)\{1 + h\alpha(1-c)x_n\}x_n}{[(1 + rt + \frac{rtx_n}{k})\{1 + h\alpha(1-c)x_n\} + t\alpha(1-c)y_n]}, \\ y_{n+1} &= \frac{[1 + (h + 2t\theta)\alpha(1-c)x_{n+1}]y_n}{[(1 + td)\{1 + h\alpha(1-c)x_{n+1}\} + t\theta\alpha(1-c)x_{n+1}]}.\end{aligned}\quad (3.4)$$

Since $0 < c < 1$ and all other parameters are positive, all solutions of the discrete-time system (3.4) remains positive for any stepsize if they start with positive initial values. Therefore, the system (3.4) is positive.

3.1.1 Existence and Stability of Fixed Points

At the fixed point, we have $x_{n+1} = x_n = x$ and $y_{n+1} = y_n = y$. From (3.3), the fixed points are obtained by solving the following couple of equations:

$$\begin{aligned}r(2x - x) - \frac{rx^2}{k} - \frac{\alpha(1-c)xy}{1 + \alpha h(1-c)x} &= 0, \\ \frac{\theta\alpha(1-c)x(2y - y)}{1 + \alpha h(1-c)x} - dy &= 0.\end{aligned}$$

We thus get three fixed points. The trivial fixed point $E_0(0, 0)$, the predator-free fixed point $E_1(k, 0)$ and the coexistence fixed point $E^*(x^*, y^*)$, where

$$\begin{aligned}x^* &= \frac{d}{\alpha(1-c)(\theta - hd)}, \\ y^* &= \frac{r(k - x^*)[1 + h\alpha(1-c)x^*]}{k\alpha(1-c)}.\end{aligned}$$

Observe that the first two fixed points always exist, but the interior fixed point exists if $\theta > hd$ and $c < c_0$, where $c_0 = 1 - \frac{d}{k\alpha(\theta - hd)}$. To show the local stability, we express the system (3.4) for convenience as

$$\begin{aligned}x_{n+1} &= f(x_n, y_n), \\ y_{n+1} &= g(x_{n+1}, y_n) = h(x_{n+1})y_n,\end{aligned}\quad (3.5)$$

where

$$\begin{aligned}
 f(x_n, y_n) &= \frac{(1 + 2rt)\{1 + h\alpha(1 - c)x_n\}x_n}{[(1 + rt + \frac{rtx_n}{k})\{1 + h\alpha(1 - c)x_n\} + t\alpha(1 - c)y_n]}, \\
 g(x_{n+1}, y_n) &= \frac{[1 + (h + 2t\theta)\alpha(1 - c)x_{n+1}]y_n}{[(1 + td)\{1 + h\alpha(1 - c)x_{n+1}\} + t\theta\alpha(1 - c)x_{n+1}]}, \\
 h(x_{n+1}) &= \frac{[1 + (h + 2t\theta)\alpha(1 - c)x_{n+1}]}{[(1 + td)\{1 + h\alpha(1 - c)x_{n+1}\} + t\theta\alpha(1 - c)x_{n+1}]}.
 \end{aligned} \tag{3.6}$$

The variational matrix of the system (3.5) is given by

$$J(x, y) = \begin{pmatrix} a_{11} & a_{12} \\ a_{21} & a_{22} \end{pmatrix},$$

where

$$\begin{aligned}
 a_{11} &= \frac{\partial f(x_n, y_n)}{\partial x_n} \\
 &= \frac{(1 + 2rt)\{1 + h\alpha(1 - c)x_n\}}{[(1 + rt + \frac{rtx_n}{k})\{1 + \alpha(1 - c)x_n\} + t\alpha(1 - c)y_n]} \\
 &\quad + \frac{(1 + 2rt)h\alpha(1 - c)x_n}{[(1 + rt + \frac{rtx_n}{k})\{1 + h\alpha(1 - c)x_n\} + t\alpha(1 - c)y_n]} \\
 &\quad - \frac{(1 + 2rt)\{1 + h\alpha(1 - c)x_n\}x_n[\frac{rt}{k} + (1 + rt)h\alpha(1 - c) + \frac{2rth\alpha(1-c)x_n}{k}]}{[(1 + rt + \frac{rtx_n}{k})\{1 + h\alpha(1 - c)x_n\} + t\alpha(1 - c)y_n]^2}, \\
 a_{12} &= \frac{\partial f(x_n, y_n)}{\partial y_n} \\
 &= \frac{(1 + 2rt)\{1 + h\alpha(1 - c)x_n\}x_nt\alpha(1 - c)}{[(1 + rt + \frac{rtx_n}{k})\{1 + h\alpha(1 - c)x_n\} + t\alpha(1 - c)y_n]^2}, \\
 a_{21} &= \frac{\partial g(x_{n+1}, y_n)}{\partial x_n} \\
 &= \frac{\partial g(x_{n+1}, y_n)}{\partial x_{n+1}} \frac{\partial f(x_n, y_n)}{\partial x_n} \\
 &= \frac{\partial g(x_{n+1}, y_n)}{\partial x_{n+1}} a_{11} \\
 &= \left[\frac{(h + 2t\theta)\alpha(1 - c)y_n}{[(1 + td)\{1 + h\alpha(1 - c)x_{n+1}\} + t\theta\alpha(1 - c)x_{n+1}]} \right. \\
 &\quad \left. - \frac{[1 + (h + 2t\theta)\alpha(1 - c)x_{n+1}]y_n[(1 + td)\alpha h(1 - c) + t\theta\alpha(1 - c)]}{[(1 + td)\{1 + h\alpha(1 - c)x_{n+1}\} + t\theta\alpha(1 - c)x_{n+1}]^2} \right] a_{11}, \\
 a_{22} &= h(x_{n+1}) + \frac{\partial g(x_{n+1}, y_n)}{\partial x_{n+1}} \frac{\partial f(x_n, y_n)}{\partial y_n} \\
 &= h(x_{n+1}) + \frac{\partial g(x_{n+1}, y_n)}{\partial x_{n+1}} a_{12} \\
 &= h(x_{n+1}) + \left[\frac{(h + 2t\theta)\alpha(1 - c)y_n}{[(1 + td)\{1 + h\alpha(1 - c)x_{n+1}\} + t\theta\alpha(1 - c)x_{n+1}]} \right. \\
 &\quad \left. - \frac{[1 + (h + 2t\theta)\alpha(1 - c)x_{n+1}]y_n[(1 + td)\alpha h(1 - c) + t\theta\alpha(1 - c)]}{[(1 + td)\{1 + h\alpha(1 - c)x_{n+1}\} + t\theta\alpha(1 - c)x_{n+1}]^2} \right] a_{12}.
 \end{aligned} \tag{3.7}$$

If λ_1 and λ_2 be the eigenvalues of the above variational matrix, we then have the following definition in relation to the stability of system (3.5).

Definition 3.1. A fixed point (x, y) of the system (3.5) is called stable if $|\lambda_1| < 1$, $|\lambda_2| < 1$ and a source if $|\lambda_1| > 1$, $|\lambda_2| > 1$. It is called a saddle if $|\lambda_1| < 1$, $|\lambda_2| > 1$ or $|\lambda_1| > 1$, $|\lambda_2| < 1$ and a nonhyperbolic fixed point if either $|\lambda_1| = 1$ or $|\lambda_2| = 1$.

Lemma 3.2 (See [40]). *Let λ_1 and λ_2 be the eigenvalues of the variational matrix*

$$J(x, y) = \begin{pmatrix} a_{11} & a_{12} \\ a_{21} & a_{22} \end{pmatrix}.$$

Then $|\lambda_1| < 1$ and $|\lambda_2| < 1$ iff the following conditions hold:

(i) $1 - \det(J) > 0$, (ii) $1 - \text{trace}(J) + \det(J) > 0$ and (iii) $0 < a_{11} < 1$, $0 < a_{22} < 1$.

Theorem 3.3. (a) *The fixed point E_0 is always a saddle point. It can't be a source or hyperbolic or even stable.*

(b) *The fixed point E_1 is stable if $c > c_0$ and it can not be a source. It is a saddle point if $c < c_0$ and there may exist a saddle-node bifurcation in the neighborhood of $c = c_0$.*

(c) *The coexistence fixed point E^* is stable if*

$$\alpha > \frac{(1 + hd)}{kh(1 - hd)}, \frac{hd(\alpha kh + 1)}{(\alpha kh - 1)} < \theta < 1 \text{ and } c_1 < c < c_0,$$

$$\text{where } c_1 = 1 - \frac{\theta + hd}{\alpha kh(\theta - hd)}, c_0 = 1 - \frac{d}{k\alpha(\theta - hd)}.$$

Proof. At the fixed point $E_0(0, 0)$, $x_{n+1} = x_n = 0$ and $y_{n+1} = y_n = 0$. The corresponding variational matrix is given by

$$J(0, 0) = \begin{pmatrix} 1 + \frac{rt}{1 + rt} & 0 \\ 0 & \frac{1}{1 + td} \end{pmatrix}.$$

So eigenvalues of $J(0, 0)$ are $\lambda_1 = 1 + \frac{rt}{1 + rt}$ and $\lambda_2 = \frac{1}{1 + td}$. Since $|\lambda_1| > 1$ and $|\lambda_2| < 1$ for all $t > 0$, the fixed point E_0 is always a saddle point and it can't be a source or a hyperbolic fixed point or even stable.

At the fixed point E_1 , the variational matrix is

$$J(k, 0) = \begin{pmatrix} a_{11} & a_{12} \\ a_{21} & a_{22} \end{pmatrix},$$

where $a_{11} = 1 - \frac{rt}{1 + 2rt}$, $a_{12} = -\frac{tk\alpha(1 - c)}{(1 + 2rt)\{1 + kh\alpha(1 - c)\}}$, $a_{21} = 0$ and $a_{22} = \frac{[1 + k\alpha(1 - c)(h + 2t\theta)]}{[(1 + td)\{1 + kh\alpha(1 - c)\} + t\theta\alpha(1 - c)]k}$. The eigenvalues of the matrix $J(k, 0)$ are $\lambda_1 = a_{11}$ and $\lambda_2 = a_{22}$. Observe that $\lambda_1 = 1 - \frac{rt}{1 + 2rt}$ is always less than unity for any step size $t > 0$ and $\lambda_2 = \frac{[1 + k\alpha(1 - c)(h + 2t\theta)]}{(1 + td)(1 + kh\alpha(1 - c)) + t\theta\alpha(1 - c)k}$ is always positive. Thus, for any $t > 0$, $\lambda_2 < 1$ if $c > c_0$, where $c_0 = 1 - \frac{d}{k\alpha(\theta - hd)}$. Clearly, the fixed point E_1 is stable if $c > c_0$. In this case, however, E^* does not exist. Since λ_1 is always less than unity, so E_1 can not be a source. On the other hand, $\lambda_2 > 1$ if $c < c_0$. Therefore, the fixed point E_1 is saddle if $c < c_0$. In this case E^* exists. The fixed point E_1 is non-hyperbolic if $c = c_0$, where $\lambda_2 = 1$. Since λ_1 and λ_2 are always positive and none of them can be equal to -1 , so period doubling bifurcation, i.e., flip bifurcation can not occur at the fixed point E_1 . When $c = c_0$ then one of the eigenvalues is 1 and the other one is neither $+1$ nor -1 . Therefore, saddle–node bifurcation may occur when parameter c is in the neighborhood of c_0 .

At the interior fixed point, $x_{n+1} = x_n = x^*$ and $y_{n+1} = y_n = y^*$. The corresponding variational matrix is

$$J(x^*, y^*) = \begin{pmatrix} a_{11} & a_{12} \\ a_{21} & a_{22} \end{pmatrix}, \text{ where}$$

$$a_{11} = 1 - \frac{rtx^*A}{kG(x^*, y^*)(\theta - hd)}, a_{12} = -\frac{t\alpha(1 - c)x^*}{G(x^*, y^*)}, a_{21} = \frac{t\alpha(1 - c)(\theta - hd)y^*}{H(x^*, y^*)}a_{11},$$

$$a_{22} = 1 + \frac{t\alpha(1 - c)(\theta - hd)y^*}{H(x^*, y^*)}a_{12}, G(x^*, y^*) = \frac{\theta(1 + 2rt)}{(\theta - hd)}, H(x^*, y^*) = \frac{\theta(1 + 2td)}{(\theta - hd)},$$

$$A = \theta + hd - kh\alpha(1 - c)(\theta - hd).$$

Since $0 < \theta < 1$ and $\theta > hd$, $G(x^*, y^*)$ and $H(x^*, y^*)$ are always positive. Thus, $1 - \text{trace}(J) + \det(J) = \frac{t^2\alpha^2(1 - c)^2(\theta - hd)x^*y^*}{G(x^*, y^*)H(x^*, y^*)}$ is positive and the condition (ii) of Lemma 3.1 is satisfied. After some algebraic computations, a_{11} can be expressed as $a_{11} = 1 - \left(\frac{rt}{1 + 2rt}\right)\left(\frac{x^*}{k}\right)\left(\frac{A}{\theta}\right)$. It is easy to observe that whenever $0 < A < \theta$ holds then $0 < a_{11} < 1$. The condition $\theta > A$ holds if $c < c_0$, which is the existence condition of E^* , and the condition $A > 0$ is satisfied if $c > c_1$. Straightforward calculation gives $a_{22} = 1 - \left(\frac{rt}{1 + 2rt}\right)\left(\frac{dt}{1 + 2dt}\right)\left(\frac{\theta - hd}{\theta}\right)\left(\frac{k - x^*}{k}\right)$. Using existence conditions of E^* , one can verify that $0 < a_{22} < 1$. Therefore, condition (iii) of Lemma 3.1 is satisfied if $c > c_1$. One can easily deduce that $1 - \det(J) = \frac{rtx^*A}{kG(x^*, y^*)(\theta - hd)}$, and it is positive if $A > 0$, i.e., if $c > c_1$. Since $0 < c < 1$, it will be more significant if we assume $c_1 > 0$ and it holds if $\frac{hd(\alpha kh + 1)}{(\alpha kh - 1)} < \theta < 1$, $\alpha > \frac{(1 + hd)}{kh(1 - hd)}$. Therefore, the

interior fixed point exists and becomes stable if conditions of the Theorem (3.3) (c) are satisfied. Hence the theorem. \square

3.1.2 Hopf Bifurcation

We already have, when $c = c_1$ then $\det J(x^*, y^*) = 1$ and $0 < \text{trace}(J) < 2$ in the neighborhood of $c = c_1$. Eigenvalues of $J(x^*, y^*)$ are complex conjugate with modulus 1 when $c = c_1$ and are given by $\lambda_{1,2} = \frac{-\text{trace}(J) \pm i\sqrt{4 - \text{trace}(J)^2}}{2}$. So, the system may experience a Hopf bifurcation at E^* in the neighborhood of $c = c_1$. The model (3.4) under a perturbation c^* at $c = c_1$ becomes

$$\begin{aligned}x_{n+1} &= \bar{f}(x_n, y_n), \\y_{n+1} &= \bar{g}(x_n, y_n),\end{aligned}\tag{3.8}$$

where

$$\bar{f}(x_n, y_n) = \frac{[1 + 2rt][1 + h\alpha(1 - c_1 - c^*)x_n]x_n}{[(1 + rt + \frac{rtx_n}{k})(1 + h\alpha(1 - c_1 - c^*)x_n) + t\alpha(1 - c - c^*)y_n]},$$

$$\bar{g}(x_n, y_n) = \frac{[1 + (h + 2t\theta)\alpha(1 - c - c^*)x_{n+1}]y_n}{[(1 + td)(1 + h\alpha(1 - c_1 - c^*)x_{n+1}) + t\theta\alpha(1 - c - c^*)x_{n+1}]}, \quad |c^*| \ll 1.$$

Let $u(n) = x(n) - x^*$ and $v(n) = y(n) - y^*$ in the model (3.8), then we transform the fixed point E^* of the map (3.4) into origin. Expanding $\bar{f}(x_n, y_n)$ and $\bar{g}(x_n, y_n)$ as a Taylor series at $(u,v)=(0,0)$ to the 2nd order, we have

$$\begin{aligned}u_{n+1} &= a_{11}u_n + a_{12}v_n + b_1u_n^2 + b_2u_nv_n + b_3v_n^2 + o((|u_n| + |v_n|)^3), \\v_{n+1} &= a_{21}u_n + a_{22}v_n + c_1u_n^2 + c_2u_nv_n + c_3v_n^2 + o((|u_n| + |v_n|)^3),\end{aligned}\tag{3.9}$$

where, $a_{11} = \frac{\delta \bar{f}(x^*, y^*, 0)}{\delta x_n}$, $a_{12} = \frac{\delta \bar{f}(x^*, y^*, 0)}{\delta y_n}$, $b_1 = \frac{1}{2} \frac{\delta^2 \bar{f}(x^*, y^*, 0)}{\delta x_n^2}$,
 $b_2 = \frac{1}{2} \frac{\delta^2 \bar{f}(x^*, y^*, 0)}{\delta x_n \delta y_n}$, $b_3 = \frac{1}{2} \frac{\delta^2 \bar{f}(x^*, y^*, 0)}{\delta y_n^2}$, $a_{21} = \frac{\delta \bar{g}(x^*, y^*, 0)}{\delta x_n}$, $a_{22} = \frac{\delta \bar{g}(x^*, y^*, 0)}{\delta y_n}$,
 $c_1 = \frac{1}{2} \frac{\delta^2 \bar{g}(x^*, y^*, 0)}{\delta x_n^2}$, $c_2 = \frac{1}{2} \frac{\delta^2 \bar{g}(x^*, y^*, 0)}{\delta x_n \delta y_n}$, $c_3 = \frac{1}{2} \frac{\delta^2 \bar{g}(x^*, y^*, 0)}{\delta y_n^2}$.

The characteristic equation associated with the linearization of (3.9) at $(u_n, v_n) = (0, 0)$ is given by

$$\lambda^2 + p(c^*)\lambda + q(c^*) = 0,\tag{3.10}$$

where

$$p(c^*) = -2 + \frac{rtd[\theta + hd - k\alpha h\{1 - (c_1 + c^*)\}(\theta - hd)]}{k\theta(1 + 2rt)\alpha\{1 - (c_1 + c^*)\}(\theta - hd)}$$

$$\begin{aligned}
 & + \frac{rt^2d(\theta - hd)}{k\theta(1 + 2rt)(1 + 2dt)} \left[k - \frac{d}{\alpha\{1 - (c_1 + c^*)\}(\theta - hd)} \right], \\
 q(c^*) & = 1 - \frac{rtd[\theta + hd - k\alpha h\{1 - (c_1 + c^*)\}(\theta - hd)]}{k\theta(1 + 2rt)\alpha\{1 - (c_1 + c^*)\}(\theta - hd)}.
 \end{aligned}$$

The roots of the characteristic equation (3.10) are

$$\lambda_{1,2} = \frac{-p(c^*) \pm i\sqrt{4q(c^*) - p^2(c^*)}}{2}.$$

Therefore, $|\lambda_{1,2}| = (q(c^*))^{\frac{1}{2}}$. Since $q(c^*) = 1$ when $c^* = 0$, we have $|\lambda_{1,2}| = 1$ at $c^* = 0$. Consequently,

$$l = \left(\frac{d|\lambda_{1,2}|}{dc^*} \right)_{c^*=0} = -\frac{1}{2} \frac{k\alpha rth^2d(\theta - hd)}{\theta(1 + 2rt)(\theta + hd)} \neq 0. \quad (3.11)$$

Also, at $c^* = 0$

$$\lambda_{1,2}^m \neq 1 \quad (3.12)$$

for $m = 1, 2, 3, 4$, which is equivalent to $p(0) \neq -2, -1, 0, 1, 2$. Since $0 < p(0) = -2 + \left(\frac{rt}{1 + 2rt} \right) \left(\frac{dt}{1 + 2dt} \right) \left(\frac{\theta - hd}{\theta} \right) \left(\frac{k - \frac{d}{\alpha(1 - c_1)(\theta - hd)}}{k} \right) < 2$, $p(0)$ can not be $-2, -1, 0, -2, 1$, because each of the four fractions is less than unity. Next we study the normal form of (3.9) when $c^* = 0$.

Let $\alpha = \text{Re}(\lambda)$ and $\beta = \text{Im}(\lambda)$. We construct an invertible matrix

$$T = \begin{pmatrix} a_{12} & 0 \\ \alpha - a_{11} & -\beta \end{pmatrix} \text{ and consider the translation } \begin{pmatrix} u_n \\ v_n \end{pmatrix} = T \begin{pmatrix} X_n \\ Y_n \end{pmatrix}.$$

Thus, the map (3.9) becomes

$$\begin{pmatrix} X_n \\ Y_n \end{pmatrix} \rightarrow \begin{pmatrix} \alpha & -\beta \\ \beta & \alpha \end{pmatrix} \begin{pmatrix} X_n \\ Y_n \end{pmatrix} + \begin{pmatrix} F(X_n, Y_n) \\ G(X_n, Y_n) \end{pmatrix},$$

where $F(X_n, Y_n) = \frac{-\beta}{\det(T)} [\{b_1a_{12}^2 + b_2a_{12}(\alpha - a_{11}) + b_3(\alpha - a_{11})^2\}X_n^2 + \{-\beta b_2a_{12} - 2b_3\beta(\alpha - a_{11})\}X_nY_n + b_3\beta^2Y_n^2 + o(u_n + v_n)^3]$, $G(X_n, Y_n) = \frac{1}{\det(T)} [\{B_1a_{12}^2 + B_2(\alpha - a_{11})a_{12} + B_3(\alpha - a_{11})^2\}X_n^2 + \{-B_2a_{12}\beta - 2B_3\beta(\alpha - a_{11})\}X_nY_n - B_3\beta Y_n^2 + o(u_n + v_n)^3]$, $B_1 = b_1(-\alpha + a_{11}) + a_{12}c_1$, $B_2 = b_2(-\alpha + a_{11}) + a_{12}c_2$, $B_3 = b_3(-\alpha + a_{11}) + a_{12}c_3$.

In order to undergo Hopf bifurcation, we require that the following discriminatory quantity s be nonzero

$$s = -\text{Re} \left[\frac{(1 - 2\bar{\lambda})\bar{\lambda}^2}{(1 - \lambda)} \xi_{11}\xi_{20} \right] - \frac{1}{2} (|\xi_{11}|^2 + |\xi_{02}|^2 + \text{Re}(\bar{\lambda}\xi_{21})),$$

where

$$\xi_{20} = \frac{1}{8} [F_{XX} - G_{YY} + 2G_{XY} + i(G_{XX} - G_{YY} - 2F_{XY})],$$

$$\begin{aligned}
\xi_{11} &= \frac{1}{4}[F_{XX} + F_{YY} + i(G_{XX} + G_{XY})], \\
\xi_{02} &= \frac{1}{8}[F_{XX} - F_{YY} + 2G_{XY} + i(G_{XX} - G_{YY} - 2F_{XY})], \\
\xi_{21} &= \frac{1}{16}[F_{XXX} + F_{XYY} + G_{XXY} + G_{YYX} + i(G_{XXX} + G_{XYY} - F_{XXY} - F_{YYX})], \\
F_{XX} &= -\frac{2\beta}{\det(T)}[b_1a_{12}^2 + b_2a_{12}(\alpha - a_{11}) + b_3(\alpha - a_{11})^2], \\
F_{XY} &= \frac{\beta}{\det(T)}[\beta b_2a_{12} + 2b_3\beta(\alpha - a_{11})], \\
F_{YY} &= -\frac{2\beta}{\det(T)}[b_3\beta^2], \\
G_{XX} &= \frac{2}{\det(T)}[B_1a_{12}^2 + B_2(\alpha - a_{11})a_{12} + B_3(\alpha - a_{11})^2], \\
G_{XY} &= -\frac{1}{\det(T)}[B_2a_{12}\beta + 2B_3\beta(\alpha - a_{11})], \\
G_{YY} &= -\frac{B_3\beta}{\det(T)}, \\
F_{XXX} &= G_{YYX} = F_{XXY} = G_{XXY} = F_{XYY} = G_{XYY} = 0.
\end{aligned}$$

Thus, from the above analysis and from Guckenheimer and Holmes [19, Theorem 3.5.2], we have the following theorem.

Theorem 3.4. *If the conditions (3.11) and (3.12) hold and $s \neq 0$, then the model system (3.4) undergoes a Hopf bifurcation at $E^*(x^*, y^*)$ when the parameter c^* varies in a small neighborhood of the origin. Moreover, if $s < 0$ (respectively $s > 0$), then an attracting (respectively repelling) invariant closed curve bifurcates from $E^*(x^*, y^*)$ for $c^* > 0$ (respectively $c^* < 0$).*

3.2 The Euler Forward Method

By Euler's forward method, we transform the continuous model (1.2) in the following discrete model:

$$\begin{aligned}
\frac{x_{n+1} - x_n}{t} &= x_n \left[r \left(1 - \frac{x_n}{k} \right) - \frac{\alpha(1-c)y_n}{1 + \alpha h(1-c)x_n} \right], \\
\frac{y_{n+1} - y_n}{t} &= y_n \left[\frac{\theta\alpha(1-c)x_n}{1 + \alpha h(1-c)x_n} - d \right],
\end{aligned} \tag{3.13}$$

where $t > 0$ is the step size. Rearranging the above equations, we have

$$\begin{aligned}
x_{n+1} &= x_n + tx_n \left[r \left(1 - \frac{x_n}{k} \right) - \frac{\alpha(1-c)y_n}{1 + \alpha h(1-c)x_n} \right], \\
y_{n+1} &= y_n + ty_n \left[\frac{\theta\alpha(1-c)x_n}{1 + \alpha h(1-c)x_n} - d \right].
\end{aligned} \tag{3.14}$$

It is to be noticed that the system (3.14) with positive initial values is not unconditionally positive due to the presence of negative terms. The system may therefore exhibit spurious behaviors and numerical instabilities.

3.2.1 Existence and Stability of Fixed Points

At fixed point, we substitute $x_{n+1} = x_n = x$ and $y_{n+1} = y_n = y$. One can easily compute that (3.14) has the same fixed points as in the previous case. The fixed point $E_0(0, 0)$, $E_1(k, 0)$ always exist and the fixed point $E^*(x^*, y^*)$ exists if $\theta > hd$ and $c < c_0$, where $x^* = \frac{d}{\alpha(1-c)(\theta-hd)}$, $y^* = \frac{r(k-x^*)[1+h\alpha(1-c)x^*]}{k\alpha(1-c)}$ and $c_0 = 1 - \frac{d}{k\alpha(\theta-hd)}$.

The variational matrix of the system (3.14) at any arbitrary fixed point (x, y) is given by

$$J(x, y) = \begin{pmatrix} a_{11} & a_{12} \\ a_{21} & a_{22} \end{pmatrix},$$

$$\text{where } a_{11} = 1 + t \left[r \left(1 - \frac{x}{k} \right) - \frac{\alpha(1-c)y}{1 + \alpha h(1-c)x} \right] + tx \left[-\frac{r}{k} + \frac{h\alpha^2(1-c)^2 y}{\{1 + \alpha h(1-c)x\}^2} \right],$$

$$a_{12} = -\frac{t\alpha(1-c)x}{1 + \alpha h(1-c)x}, \quad a_{21} = \frac{t\theta\alpha(1-c)y}{1 + \alpha h(1-c)x} - \frac{t\theta\alpha^2(1-c)^2 xy}{[1 + \alpha h(1-c)x]^2}, \quad a_{22} = 1 + t \left[\frac{\theta\alpha(1-c)x}{1 + \alpha h(1-c)x} - d \right].$$

Theorem 3.5. (a) *The equilibrium point E_0 is always unstable. It will be a saddle point if $t < \frac{2}{d}$ and a source if $t > \frac{2}{d}$.*

(b) *The equilibrium point E_1 is stable if $c > c_0$ and*

$$t < \min \left\{ \frac{2}{r}, \frac{2\{1 + k\alpha h(1-c)\}}{d - k\alpha(1-c)(\theta-hd)} \right\}.$$

It is a saddle point if $c > c_0$ and $\frac{2\{1 + k\alpha h(1-c)\}}{[d - k\alpha(1-c)(\theta-hd)]} < t < \frac{2}{r}$; or $c > c_0$

and $\frac{2}{r} < t < \frac{2\{1 + k\alpha h(1-c)\}}{[d - k\alpha(1-c)(\theta-hd)]}$.

It is a source if $c > c_0$ and $t > \max \left\{ \frac{2}{r}, \frac{2\{1 + k\alpha h(1-c)\}}{d - k\alpha(1-c)(\theta-hd)} \right\}$.

(c) *Suppose that the interior fixed point E^* exists. It is then locally asymptotically stable if $c_1 < c < c_0$ and $t < \min \left[\frac{G}{H}, \frac{2}{G} \right]$, where $G = \frac{rx^*}{k\theta}[\theta + hd - kh\alpha(1-c)(\theta-hd)]$, $H = \frac{rx^*}{k}[k\alpha(1-c)(\theta-hd) - d]$.*

Proof. At the equilibrium point E_0 , the variational matrix reads as

$$J(0, 0) = \begin{pmatrix} 1 + rt & 0 \\ 0 & 1 - td \end{pmatrix}.$$

The eigenvalues are $\lambda_1 = 1 + rt$ and $\lambda_2 = 1 - td$. Since one eigenvalue is greater than unity, E_0 is always unstable. Note that $|\lambda_2| < 1$ if $t < \frac{2}{d}$ and $|\lambda_2| > 1$ if $t > \frac{2}{d}$.

Therefore, E_0 is saddle if $t < \frac{2}{d}$ and a source if $t > \frac{2}{d}$.

The variational matrix evaluated at the fixed point $E_1(k, 0)$ is given by

$$J(k, 0) = \begin{pmatrix} a_{11} & a_{12} \\ a_{21} & a_{22} \end{pmatrix},$$

where

$$a_{11} = 1 - rt, a_{12} = -\frac{t\alpha(1-c)k}{1 + \alpha h(1-c)k}, a_{21} = 0$$

and

$$a_{22} = 1 + t \left[\frac{\theta\alpha(1-c)k}{1 + \alpha h(1-c)k} - d \right].$$

It is easy to observe that eigenvalues are given by

$$\lambda_1 = 1 - rt$$

and

$$\lambda_2 = 1 + t \left[\frac{\theta\alpha(1-c)k}{1 + \alpha h(1-c)k} - d \right].$$

Absolute value of these eigenvalues are less than unity if

$$t < \min \left\{ \frac{2}{r}, \frac{2\{1 + k\alpha h(1-c)\}}{d - k\alpha(1-c)(\theta - hd)} \right\}.$$

Therefore, the system (3.14) is locally asymptotically stable around E_1 if $c > c_0$ and $t < \min \left\{ \frac{2}{r}, \frac{2\{1 + k\alpha h(1-c)\}}{d - k\alpha(1-c)(\theta - hd)} \right\}$. However, the absolute value of λ_1 is greater

than unity if $t > \frac{2}{r}$ and that of λ_2 is greater than unity if $t > \frac{2\{1 + k\alpha h(1-c)\}}{d - k\alpha(1-c)(\theta - hd)}$ with $c > c_0$. Therefore, E_1 will be a source if $c > c_0$ and $c > c_0$ and

$$t > \max \left\{ \frac{2}{r}, \frac{2\{1 + k\alpha h(1-c)\}}{d - k\alpha(1-c)(\theta - hd)} \right\}.$$

The equilibrium point E_1 will be a saddle point if either of the following two conditions holds:

- (i) $\frac{2\{1 + k\alpha h(1 - c)\}}{[d - k\alpha(1 - c)(\theta - hd)]} < t < \frac{2}{r}$ & $c > c_0$; OR
- (ii) $\frac{2}{r} < t < \frac{2\{1 + k\alpha h(1 - c)\}}{[d - k\alpha(1 - c)(\theta - hd)]}$ & $c > c_0$.

At the interior equilibrium point E^* , the Jacobian matrix is evaluated as

$$J(x^*, y^*) = \begin{pmatrix} a_{11} & a_{12} \\ a_{21} & a_{22} \end{pmatrix},$$

where $a_{11} = 1 - tG$, $a_{12} = -\frac{t\alpha(1 - c)(\theta - hd)x^*}{\theta}$, $a_{21} = \frac{rt\theta(k - x^*)}{k}$, $a_{22} = 1$ and $a_{12}a_{21} = -t^2H$ with $G = \frac{rx^*}{k\theta}[\theta + hd - kh\alpha(1 - c)(\theta - hd)]$, $H = \frac{rx^*}{k}[k\alpha(1 - c)(\theta - hd) - d]$. One can compute that $\det(J) = 1 - tG + t^2H$ and $\text{trace}(J) = 2 - tG$.

The interior fixed point E^* of the system (3.14) will be locally asymptotically stable if the following three conditions are satisfied simultaneously [8]:

- (i) $1 - \det(J) > 0$, (ii) $1 - \text{trace}(J) + \det(J) > 0$, (iii) $1 + \text{trace}(J) + \det(J) > 0$.

Note that $1 - \text{trace}(J) + \det(J) = t^2H > 0$ as H is always positive following the existence conditions of E^* . Thus, condition (ii) is satisfied. To verify (i), we observe that $1 - \det(J)$ is positive if $t < \frac{G}{H}$. As the step size is positive and H is always positive, one can confer that $1 - \det(J)$ is positive if G is positive, implying $c > c_1$. Simple computations give, $1 + \text{trace}(J) + \det(J) = 2(2 - tG) + t^2H$. This expression will be positive if $0 < t < \frac{2}{G}$. Therefore, coexistence equilibrium point E^* exists and becomes stable if $c_1 < c < c_0$, $t < \min\left[\frac{G}{H}, \frac{2}{G}\right]$. Hence the theorem. \square

3.2.2 Hopf Bifurcation

We now show that the system (3.14) undergoes a Hopf bifurcation at the interior fixed point E^* if the following theorem holds.

Theorem 3.6. *Discrete system (3.14) undergoes a Hopf bifurcation at the interior fixed point E^* when $t = \frac{G}{H}$ and satisfies the transversality and nonresonance conditions.*

Proof. To prove this we have to show that the jacobian matrix $J(x^*, y^*)$ has a pair of complex conjugate eigenvalues in the neighborhood of $t = \frac{G}{H}$ and the following conditions hold:

- (i) $|\lambda_{1,2}| = 1$ if $t = \frac{G}{H}$,

- (ii) $\left. \frac{d|\lambda_{1,2}|}{dt} \right|_{t=\frac{G}{H}} \neq 0$ (transversality condition),
- (iii) $\left(\lambda_{1,2} \right)^s \neq 1$ for all $s = 1, 2, 3, 4$ (nonresonance conditions).

Eigenvalues of the jacobian matrix $J(x^*, y^*)$ are $\lambda_{1,2} = \frac{2 - tG + t\sqrt{G^2 - 4H}}{2}$. Therefore, $\lambda_{1,2}$ are complex conjugate if $G^2 - 4H < 0$, i.e., if $-2\sqrt{H} < G < 2\sqrt{H}$. Since $G = tH > 0$, the previous inequality becomes $0 < G < 2\sqrt{H}$. The modulus of $\lambda_{1,2}$ is equal to unity if $\det J = 1$, i.e., if $t = \frac{G}{H}$. Therefore, the Jacobian matrix $J(x^*, y^*)$ has complex conjugate roots with modulus one if parameters belong to the set $U = \{(r, k, \alpha, \theta, h, c, d) : 0 < G < 2\sqrt{H}, t = \frac{G}{H}\}$. Clearly, $\left. \frac{d|\lambda_{1,2}|}{dt} \right|_{t=\frac{G}{H}} = \frac{G}{2} \neq 0$.

Now $\left(\lambda_{1,2} \right)^s \neq 1$ for all $s = 1, 2, 3, 4$, which is equivalent to $\text{trace} J(x^*, y^*) \Big|_{t=\frac{G}{H}} \neq -2, -1, 0, 1, 2$. Since, $\text{Trace} J(x^*, y^*) \Big|_{t=\frac{G}{H}} = \frac{2H - G^2}{H}$ which will not be equal to $-2, -1, 0, 1, 2$ if $G^2 \neq 0, 4H, 3H, 2H, H$. From the set U , it is clear that G^2 can not be equal to 0 or $4H$. As $G = tH$ and $0 < t < 1$, G^2 can not be equal to $3H$ or $2H$ or H . Hence the theorem. \square

4 Numerical Simulations

In this section we present some numerical simulations to validate our analytic results of the NSFD discrete system (3.4) and the Euler system (3.14) with their continuous counterpart (1.2). For this experiment, we consider the following parameters set of the well studied predator-prey interaction *Paramecium aurelia* and *Didinium nasutum* as considered in [5]:

$$r = 2.65, K = 898, h = 0.0437, \alpha = 0.045, d = 1.06, \theta = 0.215.$$

The step size is kept fixed as $t = 0.1$ in all simulations, if not stated otherwise. We consider the initial values $I_1 = (15, 5.83)$ and $I_2 = (45, 15)$, as it were in the experimental setup [31] and [44], respectively. We consider few other initial values $I_3 = (800, 70)$, $I_4 = (700, 140)$ and $I_5 = (50, 160)$ for further verification. For the above parameter set, we find different critical values of c as $c_1 = 0.1227$, $c_0 = 0.8445$. The interior fixed point and predator-free fixed points are evaluated as $E^* = (x^*, y^*) = (253.9056, 121.8967)$ and $E_1 = (898, 0)$. We first reproduce the bifurcation diagram (Fig. 4.1) of the continuous system (1.2) with respect to the parameter c as in [5] by using ODE45 of the software Matlab 7.11.

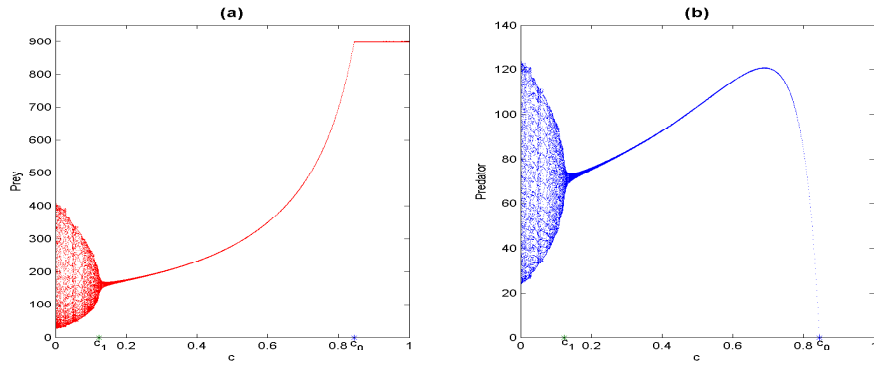


Figure 4.1: Bifurcation diagrams of system populations (1.2) with c as the bifurcation parameter. These figures show that both the prey and predator populations are unstable for $c \in [0, c_1)$ and stable for $c \in (c_1, c_0)$. Prey populations reaches to its carrying capacity and predator populations go to extinction if $c > c_0$. Parameters are $r = 2.65, K = 898, h = 0.0437, \alpha = 0.045, d = 1.06$ and $\theta = 0.215$. Here $c_1 = 0.1227$ and $c_0 = 0.8445$.

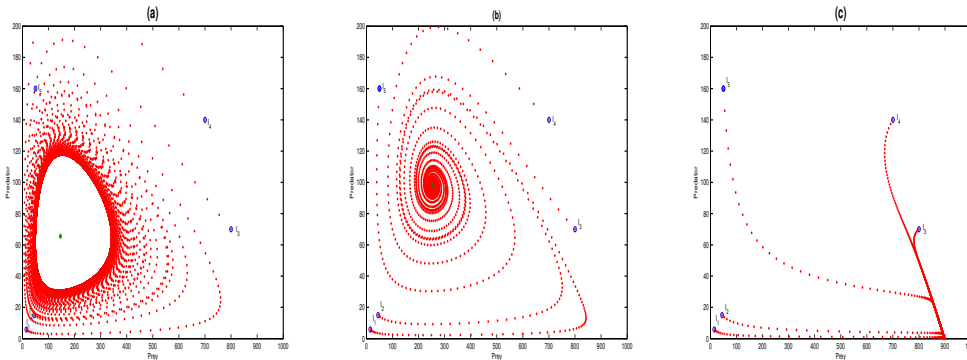


Figure 4.2: Profiles of prey and predator populations of NSFD system (3.4) for $c = 0.04$ (Fig. a), $c = 0.45$ (Fig. b) and $c = 0.85$ (Fig. c). Here time step is $t = 0.1$ and other parameters are as in the Fig. 4.1.

Following the analytical results stated in Section 2, the bifurcation diagrams show that the equilibrium E^* is unstable for $0 < c < c_1$ and stable for $c_1 < c < c_0$. The predator-free equilibrium E_1 is stable for $c > c_0$. Thus, all species coexist in stable state at intermediate degree of complexity ($c_1 < c < c_0$) and coexist in oscillatory state at lower degree of complexity ($0 < c < c_1$). Predator population goes to extinction and the prey population reaches to its carrying capacity at higher degree of complexity $c > c_0$.

Representative behavior of trajectories of the NSFD system (3.4) for low ($0 < c < c_1$), intermediate ($c_1 < c < c_0$) and high ($c > c_1$) structural complexity are presented

in the Fig. 4.2. The first figure (Fig. 4.2a) shows that solutions starting from different initial points converge to the stable limit cycle for lower value of $c = 0.04$. All solutions converge to the stable coexistence equilibrium E^* for intermediate value of $c = 0.45$ (Fig. 4.2b). However, the predator population goes to extinction and the prey population reaches to its carrying capacity at higher value of $c = 0.85$ (Fig. 4.2c), depicting the stability of the equilibrium E_1 .

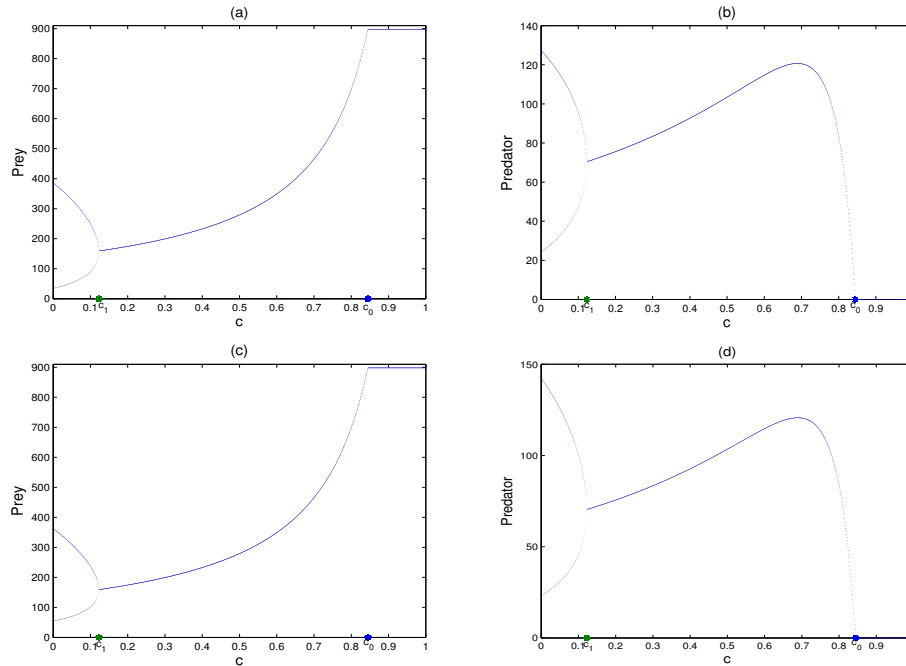


Figure 4.3: Bifurcation diagrams of prey population (Fig. a) and predator population (Fig. b) of NSFD model (3.4) with c as the bifurcation parameter with step size $t = 0.1$. The same have been plotted with step size $t = 3$ (Figs. c & d). These figures show that both the prey and predator populations oscillate for $c \in (0, c_1)$ and stable for $c \in (c_1, c_0)$. The predator-free equilibrium E_1 is stable for $c > c_0$. Figures (a) & (c) are qualitatively same; similar is the case for (b) & (d). Thus, NSFD scheme is independent of step size. All parameters are as in Fig. 4.1.

Dynamics of the system (3.4) for varying c can be succinctly represented by the bifurcation diagram Fig. 4.3. It shows that all populations oscillate for $0 < c < c_1$ and coexist in stable state for $c_1 < c < c_0$. If $c > c_0$, then predator-free equilibrium is stable. This figure shows that NSFD model (3.4) exhibit the same behavior as that of the continuous model (1.2) (compare Figs. 4.3 (a,b) with Figs.4.1 (a,b)) and therefore dynamically consistent. We have plotted the same bifurcation diagrams with step size $t = 3$ (Figs. 4.3(c), 4.3(d)). The qualitative behavior remains same in both cases, implying that NSFD scheme is independent of step size.

We plot the bifurcation diagram of Euler discrete system (3.14) in Fig. 4.4 with same

step size $t = 0.1$. It shows that stability change does not occur at the lower critical value $c = c_1$ but at a latter value of c . Thus, Euler’s scheme is not dynamically consistent with its continuous counterpart.

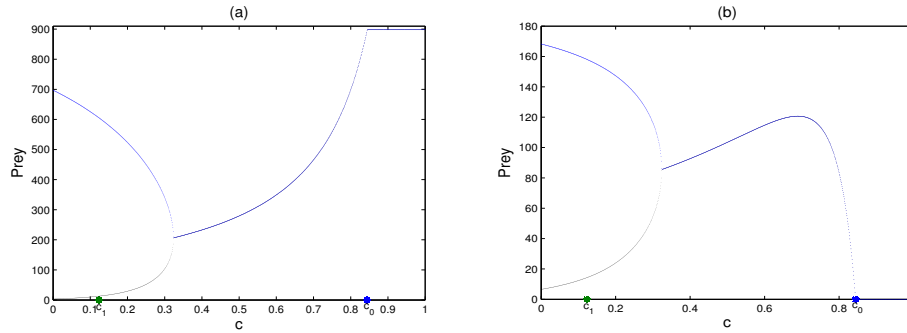


Figure 4.4: Bifurcation diagram of the prey population (Fig. 4.4a) and that of the predator population (Fig. 4.4b) in Euler’s discrete system (3.14) with step size $t = 0.1$. Parameters are as in the Fig. 4.1. Though parameters of Fig. 4.2 and Fig. 4.4 are same, populations in Fig. 4.4 stabilize at much higher value than c_1 , implying dynamic inconsistency of the system (3.14) with the original continuous system (1.2)

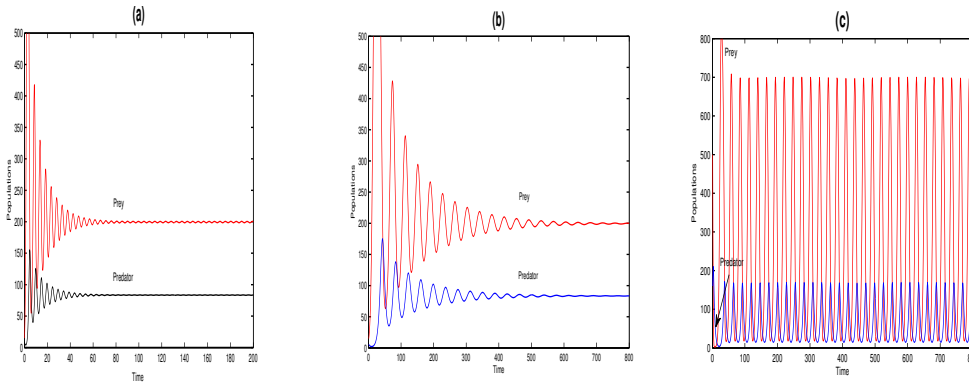


Figure 4.5: Figs. (a), (b) and (c) represent, respectively, the time series solutions of the systems (1.2), (3.4) and (3.14) for $c = 0.3$. In Figs. (b), (c) step size are taken as $t = 0.23$ and Fig. (a) is plotted by using ODE45 of Matlab 7.11. The first two figures show that both populations are stable and thus NSFD model is dynamically consistent with the continuous system. But the last figure shows that populations are unstable, indicating the inconsistency of the Euler system with its continuous counterpart.

According to the results of the continuous system (1.2), solutions should converge to the stable equilibrium E^* for the intermediate value $c = 0.3$ (Fig.4.5a). Though NSFD system (3.4) converges to the interior equilibrium E^* (Fig.4.5b), Euler discrete system

(3.14) oscillates around E^* (Fig.4.5c). These results indicate the dynamic consistency of NSFD system and inconsistency of Euler system with its continuous counterpart.

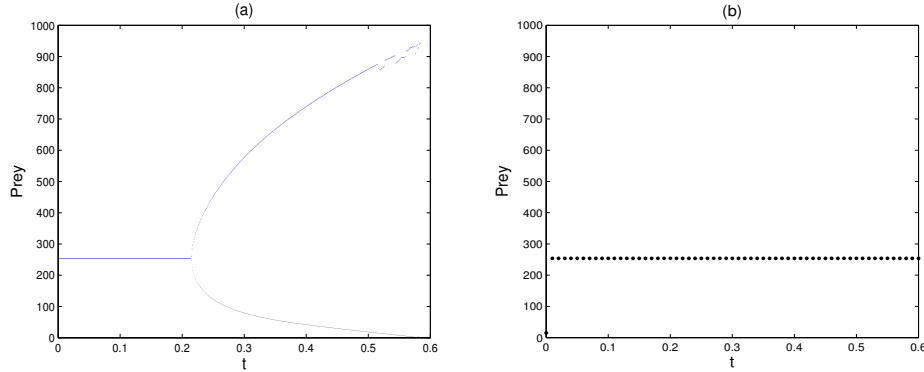


Figure 4.6: Bifurcation diagrams of prey population of Euler forward model (3.14) (Fig. a) and NSFD model (3.4) (Fig. b) with stepsize t as the bifurcation parameter. Here $c = 0.45$ and all the parameters and initial point are same as in Fig. 4.1. The first figure shows that the prey population is stable for small stepsize t and unstable for higher value of t . The second figure shows that the prey population is stable for all stepsize t .

To compare stepsize dependency of the Euler model and NSFD model, we have plotted the solutions of the systems (3.14) and (3.4) considering the stepsize t as a variable parameter (Fig. 4.6) for a fixed intermediate value of $c = 0.45$. It is to be recalled (see Fig. 4.2) that the continuous system (1.2) is stable at this intermediate value of complexity, $c = 0.45$. Fig. 4.6a shows that solution behavior of Euler's model depends on the stepsize. If stepsize is small, system population is stable and it resembles with the continuous system (1.2). As stepsize is increased, system population begins to fluctuate and thus shows spurious behaviors. However the second figure (Fig. 4.6b) shows that NSFD model (3.4) remains stable for all t , indicating independency of stepsize.

5 Summary

Nonstandard finite difference method (NSFD) scheme has gained lot of attentions in the last few years because it generally does not show spurious behavior as compared to other standard finite difference methods. It can also improve the accuracy and reduce computational costs of traditional finite-difference schemes. In this work, we have studied two discrete systems by using NSFD scheme and forward Euler scheme of a well studied two-dimensional continuous predator–prey system that considers the effect of habitat complexity. We have shown that dynamics of the discrete system formulated by NSFD scheme are same as that of the continuous system. It preserves the local stability of all the fixed points and the positivity of the solutions of the continuous system for any step size. Simulation experiments show that NSFD system always converge to the

correct steady-state solutions for any arbitrary large value of step size (t) in accordance with the theoretical results. However, the discrete model formulated by forward Euler method does not show consistency with its continuous counterpart. Rather it shows scheme-dependent instability when stepsize restriction is violated.

Acknowledgement

Research of N. Bairagi is supported by DST PURSE II.

References

- [1] R. Anguelov, Y. Dumont, J.M.S. Lubumaa, M. Shillor, *Dynamically consistent nonstandard finite difference schemes for epidemiological models*, J. Computational and Appl. Maths., 255 (2014), 161–182.
- [2] R. Anguelov, J.M-S. Lubuma, *Nonstandard Finite Difference Method by Nonlocal Approximation*, Mathematics and Computers in Simulation, 61 (2003), 465–475.
- [3] P. V. August, *The role of habitat complexity and heterogeneity in structuring tropical mammal communities*, Ecology, 64 (1983), 1495–1507.
- [4] N. Bairagi, D. Jana, *Age-structured predator-prey model with habitat complexity: oscillations and control*, Dynamical Systems, 27 (2012), 475–499.
- [5] N. Bairagi, D. Jana, *On the stability and Hopf bifurcation of a delay-induced predator-prey system with habitat complexity*, Appl. Math. Modelling, 35 (2011), 3255–3267.
- [6] S. Bell, E. McCoy, H. Mushinsky, *Habitat structure: the physical arrangement of objects in space*, Chapman Hall, (1991), 3–27.
- [7] J. S. Beukers, G. P. Jones, *Habitat complexity modifies the impact of piscivores on a coral reef fish population*, Oecologia, 114 (1997), 50–59.
- [8] F. Brauer and C. Castillo-Chavez, *Mathematical models in population biology and epidemiology*, Springer-Verlag, 2001.
- [9] C.R. Canion, K.L. Heck, *Effect of habitat complexity on predation success: re-evaluating the current paradigm in seagrass beds*, Marine Eco. Prog. Series, 393 (2009), 37–46.
- [10] D. T. Dimitrov, H. V. Kojouharov, *Nonstandard finite-difference schemes for general two-dimensional autonomous dynamical systems*, Appl. Maths. Letters, 18 (2005), 769–774.

- [11] D. T. Dimitrov, H. V. Kojouharov, *Nonstandard finite-difference methods for predator-prey models with general functional response*, Math. and Compu. Simu., 78 (2008), 1–11.
- [12] D. T. Dimitrov, H.V. Kojouharov, *Positive and elementary stable nonstandard numerical methods with applications to predator-prey models*, J. Comput. Appl. Math., 189 (2006), 98–108.
- [13] D. Ding, Q. Ma, X. Ding, *A nonstandard difference scheme for an epidemic model with vaccination*, J. Diff. Equ. and Appli., 19 (2013), 179–190.
- [14] S. E. Flanders, *A host-parasite community to demonstrate balance*, Ecology, 29 (1948), 123.
- [15] S. S. Frederick, P. John, M. C. F. Manderson, *The effects of seafloor habitat complexity on survival of juvenile fishes: Species-specific interactions with structural refuge*, J. Exp. Marine Bio. and Eco., 335 (2006), 167–176.
- [16] G. F. Gause, *The Struggle for Existence*, Williams and Wilkins, Baltimore, 1934.
- [17] J. H. Grabowski, *Habitat complexity disrupts predator-prey interactions but not the trophic cascade on oyster reefs*, Ecology, 85 (2004), 995–1004.
- [18] B. Gratwicke, M. R. Speight, *Effects of habitat complexity on Caribbean marine fish assemblages*, Marine Eco. Prog. Series, 292 (2005), 301–310.
- [19] J. Guckenheimer, P. Holmes, *Nonlinear oscillations*, Dynamical systems and Bifurcations of Vector Fields, Springer-Verlag, Berlin, 1983.
- [20] Z. He, X. Lai, *Bifurcation and chaotic behavior of a discrete-time predator-prey system*, Nonlinear Analysis RWA, 12 (2011), 403–417.
- [21] Z. Hu, Z. Teng, L. Zhang, *Stability and bifurcation analysis of a discrete predator-prey model with nonmonotonic functional response*, Nonlinear Analysis RWA, 12 (2011), 2356–2377.
- [22] C. B. Huffaker, *Experimental studies on predation: dispersion factors and predator-prey oscillations*, Hilgardia, 27 (1958), 343–383.
- [23] N. E. Humphries, H. Weimerskirch, N. Queiroza, E. J. Southalla, and D. W. Sims, *Foraging success of biological Lévy flights recorded in situ*, PNAS, 109 (2011), 7169–7174.
- [24] D. Jana, N. Bairagi, *Habitat complexity, stochasticity and the stability of predator-prey interactions*, J. Control Eng. and Techn., 3 (2013), 76–83.

- [25] D. Jana, N. Bairagi, *Habitat complexity, dispersal and metapopulations: macroscopic study of a predator-prey system*, *Ecological Complexity*, 17 (2014), 131–139.
- [26] Z. Jing and J. Yang, *Bifurcation and Chaos in discrete-time predator-prey system*, *Chaos, Solitons and Fractals*, 27 (2006), 259–277.
- [27] M. P. Johnson, N. J. Frost, M. W. J. Mosley, M. F. Roberts, S. J. Hawkins, *The area-independent effects of habitat complexity on biodiversity vary between regions*, *Ecology Letters*, 6 (2003), 126–132.
- [28] M. E. Koivisto, M. Westerbom, *Habitat structure and complexity as determinants of biodiversity in blue mussel beds on sublittoral rocky shores*, *Marine Biology*, 157 (2010), 1463–1474.
- [29] J.D. Lambert, *Numerical methods for ordinary differential systems: The initial value problem*, Wiley, Chichester, 1991.
- [30] S. A. Lassau, D. F. Hochuli, *Effects of habitat complexity on ant assemblages*, *Ecography*, 27 (2004), 157–164.
- [31] L. S. Luckinbill, *Coexistence in Laboratory Populations of Paramecium aurelia and its predator Didinium nasutum*, *Ecology*, 54 (1973), 1320–1327.
- [32] R.E. Mickens, *Advances in the applications of Nonstandard Finite Difference Schemes*, World Scientific publishing, Signapore, 2005.
- [33] R. E. Mickens, *A nonstandard finite-difference scheme for the Lotka-Volterra system*, *Appl. Numer. Math.*, 45 (2003), 309–14.
- [34] R.E. Mickens, *Dynamic consistency: a fundamental principle for constructing NSFD schemes for differential equations*, *J. Diff. Equ. and Appl.*, 11 (2005), 645–653.
- [35] R.E. Mickens, *Exact solutions to a finite-difference model of a nonlinear reaction-advection equation: Implications for numerical analysis*, *Numer. Methods Partial Diff. Eq.*, 5 (1989), 313–325.
- [36] H. A. Obaid, R. Ouifki, K.C. Patidar, *An unconditionally stable nonstandard finite difference method applied to a mathematical model of HIV infection*, *Int. J. Appl. Math. Comput. Sci.*, 23 (2013), 357–372.
- [37] L. Persson, *Predator-mediated competition in prey refuges: the importance of habitat dependent prey resources*, *Oikos*, 68 (1993), 12–22.

- [38] L. Persson, S. Diehl, L. Johansson, G. Andersson, S. F. Hamrin, *Shifts in fish communities along the productivity gradient of temperate lakes-patterns and the importance of size-structured interactions*, J. Fish Biology, 38 (1991), 281–293.
- [39] L. Persson, S. Diehl, L. Johansson, G. Andersson, S. F. Hamrin, *Trophic interactions in temperate lake ecosystems: a test of food chain theory*, American Naturalist, 140 (1992), 59–84.
- [40] L-I. W. Roeger, G. Lahodny, *Dynamically consistent discrete Lotka-Volterra competition systems*, J. Diff. Equ. and Appl., 19 (2013), 191–200.
- [41] J. F. Savino, R. A. Stein, *Predator-prey interaction between largemouth bass and bluegills as influenced by simulated, submersed vegetation*, Trans. Am. Fish. Soc., 111 (1982), 255–266.
- [42] H. Su, X. Ding, *Dynamics of a nonstandard finite-difference scheme for Mackey-Glass system*, J. Math. Anal. Appl., 344 (2008), 932–41.
- [43] M. Tokeshi, S. Arakaki, *Habitat complexity in aquatic systems: fractals and beyond*, Hydrobiologia, 685 (2012), 27–47.
- [44] B.G. Veilleux, *An analysis of the predator interaction between Paramecium and Didinium*, J. Animal Ecology, 48 (1979), 487–803.
- [45] Y. Wang, *Dynamics of a nonstandard finite-difference scheme for delay differential equations with unimodal feedback*, Commun. Nonlinear. Sci. Numer. Simulations, 17 (2012), 3967–3978